

### Eocene Localities from which Shark Teeth were Analyzed

BKS 2004-1 (N73°43'; W120°49'), Muskox River; BKS 2004-13 and BKS 2004-15 (N74°10'; W120°51'), and BKS 2004-31 (N74°09'; W120°47') near Eames River; Aulavik National Park, northern Banks Island, NWT, Canada (Fig. DR1)

### Discussion of Diagenesis

The Delaware State University Shark Tagging Program (led by DAF) opportunistically collected teeth from 20 individual extant *C. taurus* during 2012 while deploying acoustic telemetry tags. We prepared these extant teeth for carbonate oxygen isotope analysis using the same methods described in the main text. The mean  $\delta^{18}\text{O}_{\text{CO}_3}$  values for extant *C. taurus* teeth was 0.5‰ and  $1\sigma = 1.4$  (DR Table 2). The mean  $\delta^{18}\text{O}_{\text{CO}_3}$  value of the Eocene Arctic sand tiger shark and extant *C. taurus* population differ, as expected due to habitat differences, but the variation between the modern and Eocene populations is similar (Eocene Arctic sand tiger shark  $1\sigma = 1.1$ ).

For XRD analysis, enameloid powder from two extant sharks and 7 early – middle Eocene sand tiger shark (*Striatolamia* and *Carcharias*) teeth were compared for crystallinity index. We sampled one extant tooth each from *C. taurus* (ST12-207, from the Delaware Bay population discussed above) and *Prionace glauca* (blue 1). The Eocene Arctic shark teeth (N=7) were selected based on the following criteria: three random individuals, individuals with high or low  $\delta^{18}\text{O}_{\text{CO}_3} - \delta^{18}\text{O}_{\text{PO}_4}$  offset (based on the criteria of Venneman et al., 2001), and root/inner dentine cavity. Additional teeth with anomalous  $\delta^{18}\text{O}_{\text{CO}_3} - \delta^{18}\text{O}_{\text{PO}_4}$  offset (9.1‰,  $1\sigma=1.5$ ; Venneman et al., 2001) would ideally be analyzed with XRD, but we were sample limited for some teeth (i.e., 2004-13 1, 2004-15 5, 2004-15E, sharktic 2). Powdered samples (~5 mg) were subjected to XRD analysis using an XDS 2000 diffractometer with a rotating sample holder and a 2.2 kW sealed copper radiation source (Dept. of Geology and Geophysics Microbeam Facility, University of Wyoming). Samples were individually analyzed over three hours, with measurements collected from 2° to 70° 2 $\theta$  at 0.2° intervals. Standards analyzed for reference with the shark enameloid were a calcium phosphate hydroxyapatite, calcium fluoride phosphate, calcium carbonate phosphate fluoride hydroxide, and a calcium chloride phosphate. The patterns of extant sharks and Eocene Arctic sand tiger shark enameloid are evaluated based on the following equation for crystallinity index (CI) from Person et al. (1995):

$$\text{CI} = \Sigma \{H[202], H[300], H[112]\}/H[211]$$

where  $H[202]$ ,  $H[300]$ ,  $H[112]$ , and  $H[211]$  are the respective peak heights related to the preceding valley.

The CI for extant sand tiger and blue shark teeth are 1.60 and 1.42, respectively, which were used as our thresholds for unaltered Eocene Arctic sand tiger shark teeth. The mean CI for Eocene Arctic shark enameloid we considered “unaltered” was 1.47 ( $N=5$ ,  $1\sigma=0.04$ , Table DR2), falling within the range of CI values for extant shark teeth. The Eocene root/dentine sample (sharktic E) had a CI of 0.54, which we considered “altered” based on the dark coloration, texture, and high organic carbon content. In addition, individuals 2004-15 1 and 2004-31 2 had enameloid CIs of 1.03 and 1.24, respectively, which were considered “altered.” However, the salinity model used an average for the Eocene Arctic population and therefore the  $\delta^{18}\text{O}_{\text{CO}_3}$  value for 2004-15 1, which was similar to the population mean, was effectively used to estimate salinity (DR Table 1 and 2). Based on the standards analyzed, shark tooth enameloid composition corresponds to calcium phosphate hydroxide and calcium carbonate phosphate fluoride hydroxide.

Phosphate and carbonate are co-precipitated within hydroxyapatite during formation (Posner et al., 1984), and previous studies identified an offset between hydroxyapatite  $\delta^{18}\text{O}$  values in phosphate and carbonate. For example, Venneman et al. (2001) reported an offset of 9.1‰ ( $1\sigma=1.5$ ) based upon analyses of teeth from 10 extant marine shark species spanning 3 Orders. We compiled  $\delta^{18}\text{O}_{\text{CO}_3}$  and  $\delta^{18}\text{O}_{\text{PO}_4}$  datasets spanning a wide range of  $\delta^{18}\text{O}$  values including mammalian teeth (Iacumin et al., 1992; Chenery et al., 2012), fossil marine invertebrates and vertebrates (Longinelli and Nuti, 1968), and extant shark teeth (Vennemann et al., 2001), with which to compare the offset of hydroxyapatite  $\delta^{18}\text{O}$  values in phosphate and carbonate in the Eocene Arctic shark teeth, and evaluate potential diagenetic alteration. Although these sample preparation methods differed, we compiled them to compare the widest range of  $\delta^{18}\text{O}_{\text{CO}_3} - \delta^{18}\text{O}_{\text{PO}_4}$  offset. The previously published datasets were used to determine a linear relationship and 95% prediction intervals; the  $\delta^{18}\text{O}_{\text{PO}_4-\text{CO}_3}$  relationship of the Eocene Arctic shark teeth fall within the 95% prediction interval (Fig. DR3), but to be conservative, we rejected samples with an offset beyond the tolerance of 7.2‰ – 11.8‰, the range of offset in modern shark tooth enameloid determined by Venneman et al. (2001).

### Isotopic Preparation and Analysis Specifics

The  $\text{Ag}_3\text{PO}_4$  preparation method we used is modified from Bassett et al. (2007) and Weidemann-Bidlack et al. (2008). Briefly, ~2mg of powdered enameloid powder were abraded using the Dremel with diamond bit at low speed. Powders were treated for 17–20 hours with 300 $\mu\text{l}$  2–3% NaOCl to remove organics, then bioapatite was dissolved overnight in 100 $\mu\text{l}$  0.5M  $\text{HNO}_3$ . The solution was neutralized and 75 $\mu\text{l}$  of 0.5M KOH

and 200µl of 0.36M were added to precipitate CaF<sub>2</sub>. The resulting supernatant was transferred to a reaction vessel and 250µl of silver amine solution were added (0.2N AgNO<sub>3</sub>, 0.35M NH<sub>4</sub>NO<sub>3</sub>, 0.74M NH<sub>4</sub>OH). Silver phosphate was precipitated overnight in a heat block (50°C), rinsed 5 times with deionized water, and dried at 50°C. Triplicates of each sample were weighed (250 – 300 µg) into silver capsules and run with a synthetic silver phosphate from Sigma-Aldrich (n = 27, 1σ < 0.4‰).

We prepared standards according to the carbonate and phosphate preparation methods. For δ<sup>18</sup>O<sub>CO3</sub> methods, phosphate rock (NBS120C) was used as a preparation standard. A previously reported δ<sup>18</sup>O<sub>CO3</sub> mean for NBS 120c is -2.3‰ (Tutken et al., 2006) and our mean was -2.2‰ (N=3, 1σ=0.04, VPDB). For δ<sup>18</sup>O<sub>PO4</sub> methods, phosphate rock (NBS120C) and a synthetic hydroxyapatite (HYD) were used as preparation standards. The reported δ<sup>18</sup>O<sub>PO4</sub> mean for NBS 120c is 22.1‰ (Vennemann et al., 2002) and our mean was 22.3‰ (N=3, 1σ=0.1). The running mean for HYD is 17.5‰ (N=30, 1σ=0.2) and the mean of HYD prepared with our samples is 17.3‰ (N=3, 1σ=0.4).

In addition to these process standards, there were also analytical standards used for data normalization. For carbonate analysis, the total variation within, and between, runs was based on three calcium carbonate reference materials (UWSIF 6, 17, and 18), which had a total variation of <0.3‰ (N=26) and are in-house standards that are calibrated regularly to LSVEC, NBS18 and NBS19. For phosphate analysis, the total variation within, and between, runs was based on the following materials: two synthetic Ag<sub>3</sub>PO<sub>4</sub> (N=29, 1σ<0.4), two benzoic acid (N=22, 1σ<0.4), and cellulose (N=21, 1σ=0.2). The Ag<sub>3</sub>PO<sub>4</sub> reference materials are from Arcos and Elemental and calibrated based on the two benzoic acids (601 and 602). Additional QA/QC protocols for carbonate and phosphate isotopic analyses are available from UWSIF upon request.

## Model Specification

To make inference on salinity  $S$ , the δ<sup>18</sup>O of the environment  $W$  in which individual  $i = \{1, \dots, n\}$  lived as measured the δ<sup>18</sup>O<sub>CO3</sub> value of shark teeth  $y_i$  was modeled as a function of salinity  $S$ , temperature  $T$ , and δ<sup>18</sup>O of freshwater inputs (i.e., precipitation)  $F$ . The physical relationships between the δ<sup>18</sup>O<sub>CO3</sub> value of shark teeth and their environmental water is as follows:

$$10^3 \ln \alpha_{\text{CaCO}_3\text{-w}} = \frac{2.78 \times 10^6}{T^2} - 2.89 \quad (1)$$

$$\alpha_{\text{CaCO}_3\text{-w}} = \frac{(\delta^{18}\text{O}_{\text{CaCO}_3} + 10^3)}{(\delta^{18}\text{O}_w + 10^3)} \quad (2)$$

where  $\alpha$  is the oxygen fractionation factor of  $\text{CaCO}_3$  as it relates to temperature ( $T$ , in K) and a ratio between the  $\delta^{18}\text{O}$  values of enameloid ( $\text{CaCO}_3$ ) to environmental water ( $w$ ) composition. An alternative model for phosphate  $\delta^{18}\text{O}$  values was based on the following equation (Longinelli and Nuti 1973; Kocsis et al. 2009):

$$T \text{ (}^\circ\text{C)} = 111.4 - 4.3 (\delta^{18}\text{O}_{\text{PO}_4} - \delta^{18}\text{O}_w) \quad (\text{DR Eqn. 1}).$$

In addition, the relationship of salinity  $S$  with isotopic values of  $\delta^{18}\text{O}$  (freshwater [ $F$ ] and environmental water [ $W$ ]), we can model  $y_i$  as a normal distribution with mean depending on  $T$ ,  $S$ , and  $F$

$$y_i \sim N\left(\left[W + 10^3\right] \times \alpha - 10^3, \sigma^2\right) \quad (\text{DR Eqn 2})$$

$$\text{where } W = \left[ S \frac{F - \beta_0}{\beta_1} + F - 30.91 \right] \times [1.03091]^{-1}, \quad (\text{DR Eqn 3})$$

$\beta_0$  and  $\beta_1$  are regression coefficients representing the relationship between the  $\delta^{18}\text{O}$  of freshwater and the slope of the relationship between  $\delta^{18}\text{O}_w$  and salinity, respectively (Fig. 2A),  $\alpha = \exp[2.78 \times 10^3(T^2) - 2.89 \times 10^{-3}]$ , and  $\sigma^2$  is the process error variance. Using independently published observations from Khim and Krantz (1996), LeGrande and Schmidt (2006, and references therein), and Waddell and Moore (2008, and references therein) for the  $\delta^{18}\text{O}$  of freshwater  $z_j$  and the slope of the relationship between  $\delta^{18}\text{O}$  of the environment ( $W$ ) and salinity ( $S$ )  $x_j$  across the world's oceans, we modeled  $\beta_0$  and  $\beta_1$  as a linear regression

$$z_j \sim N(\beta_0 + \beta_1 x_j, V^2) \quad (\text{DR Eqn 4})$$

where  $j$  is an index for the samples from this independent data  $j = \{1, \dots, J\}$  and  $V^2$  is the regression error variance.

For the process error variance, we assumed a weak inverse-gamma prior distributions  $\sigma^2 \sim \text{Gamma}^{-1}(3, 10)$  so that distribution of the prior process error variance has mean equal to 5 and variance equal to 25. For the regression variance, we assumed a somewhat stronger inverse-gamma prior distributions  $V^2 \sim \text{Gamma}^{-1}(3, 3)$  so that distribution of the prior regression error variance has mean equal to 1.5 and variance equal to 2.25. The inverse-gamma is commonly used to characterize the variance of normal distributions because it is conjugate with the normal, allowing for the variance to be sampled directly from the posterior distribution (Clark, 2007). We also assume that the

prior distributions on  $T$ ,  $S$  and  $F$  are uniform with support on differing ranges, depending on the data source (Table DR4). While the priors do differ for each of the datasets, model testing indicating that the priors did not result in qualitatively different results for estimates of salinity  $S$ . In contrast, estimates of temperature  $T$  and freshwater oxygen isotopes  $F$  were not well identified and largely reproduced the prior distribution (Table DR4 and DR5).

To estimate parameters, we used a Gibbs sampler with an adaptive Metropolis algorithm for conditional posterior parameter distributions that could not be sampled directly ( $T$ ,  $S$ ,  $F$ ,  $\beta_0$ , and  $\beta_1$ ). Posterior parameter distributions are described in detail in *Posterior Parameter Distribution Descriptions*. For each dataset and its associated set of priors (Table DR3), we ran the Gibbs sampler for 200,000 iterations. Based on visual inspection of the MCMC output, we discarded the first 100,000 iterations. To remove autocorrelation in the MCMC output, we thinned the output to every 100 iterations. Means and standard deviations for parameter estimates are given in Table DR4 and correlations between parameter estimates are provided in Figure DR4. Parameter distributions for three model variations (Eocene Arctic, Waddell and Moore [2008], and extant *C. taurus*) are given in Table DR4.

### ***Posterior Parameter Distribution Descriptions***

Conditional posterior parameter distributions were formulated based on a joint posterior distribution. In this section, we use the priors for the Eocene shark teeth as an example. Given model specification in the previous section, we can construct a joint posterior distribution

$$\begin{aligned}
 p(S, F, T, \sigma^2 | y_i, \text{priors}) \propto & \prod_{i=1}^n N\left(\left[W + 10^3\right] \times \alpha - 10^3, \sigma^2\right) \times \\
 & \prod_j N\left(z_j | \beta_0 + \beta_1 x_j, V^2\right) \times \\
 & \text{Unif}(S | 0, 25) \times \text{Unif}(F | -20, -15) \times \text{Unif}(T | 8, 13) \times \quad (\text{DR Eq. 5}) \\
 & N(\beta_0 | 1, 10) \times N(\beta_1 | 30, 100) \times \\
 & \text{Gamma}^{-1}(\sigma^2 | 3, 10) \times \text{Gamma}^{-1}(V^2 | 3, 3)
 \end{aligned}$$

Using the joint posterior distribution (DR Eqn 2), we can write the conditional posterior parameter distributions. The joint conditional posterior distribution for the process parameters  $T$ ,  $S$ , and  $F$  was

$$p(T, S, F | y_i, \beta_0, \beta_1, \sigma^2, \text{priors}) \propto \prod_i N(y_i | [W + 10^3] \times \alpha - 10^3, \sigma^2) \times \\ \text{Unif}(S | 8, 13) \times \text{Unif}(S | 0, 25) \times \text{Unif}(F | -20, -15)$$

This posterior was sampled using an adaptive Metropolis-Hastings algorithm.

The joint conditional posterior parameter distribution for regression parameters  $\beta_0$  and  $\beta_1$  was

$$p(\beta_0, \beta_1 | y_i, z_i, x_i, T, S, F, \sigma^2, V^2, \text{priors}) \propto \prod_j N(z_j | \beta_0 + \beta_1 x_j, V^2) \times \\ \prod_i N(y_i | [W + 10^3] \times \alpha - 10^3, \sigma^2) \times \\ N(\beta_0 | 1, 10) \times N(\beta_1 | 30, 100)$$

This posterior is sampled using an adaptive Metropolis-Hastings algorithm.

The conditional posterior distribution for the process error parameter  $\sigma^2$  was

$$p(\sigma^2 | T, S, F, y_i, \text{priors}) \propto \prod_{i=1}^n N(y_i | [W + 10^3] \times \alpha - 10^3, \sigma^2) \times \text{Gamma}^{-1}(\sigma^2 | 3, 10) \\ = \text{Gamma}^{-1}\left(\sigma^2 \left| \frac{n}{2} + 3, 10 + \frac{1}{2} \sum_{i=1}^n (y_i - [W + 10^3] \times \alpha - 10^3)^2 \right.\right)$$

with the process error drawn directly from the conditional posterior.

The conditional posterior distribution for the regression error parameter  $V^2$  was

$$p(V^2 | z_j, x_j, \beta_0, \beta_1, \text{priors}) \propto \prod_{i=j}^m N(z_j | \beta_0 + \beta_1 x_j, V^2) \times \text{Gamma}^{-1}(V^2 | 3, 3) \\ = \text{Gamma}^{-1}\left(\sigma^2 \left| \frac{n}{2} + 3, 3 + \frac{1}{2} \sum_{i=1}^n (y_i - [W + 10^3] \times \alpha - 10^3)^2 \right.\right)$$

with the regression error drawn directly from the conditional posterior.

**Table DR1: crown height and isotopic data from Eocene arctic sand tiger shark teeth.**

Identifier	Genus	Crown height (mm)	Carbonate <sup>a</sup>			Phosphate <sup>b</sup>		$\delta^{18}\text{O}_{\text{CO}_3} - \delta^{18}\text{O}_{\text{PO}_4}$ (VSMOW)	$\delta^{18}\text{O}_{\text{CO}_3} - \delta^{18}\text{O}_{\text{PO}_4}$ 1 $\sigma$	Data used in this study?	Anterior, Lateral, Posterior, Unknown
			Corr. $\delta^{18}\text{O}$ (VPDB)	$\delta^{18}\text{O}$ (VSMOW)	$\delta^{18}\text{O}$ 1 $\sigma$	$\delta^{18}\text{O}$ (VSMOW)	$\delta^{18}\text{O}$ 1 $\sigma$				
2004-13 1	<i>Carcharias</i>	10.9	-7.4	23.2	0.2	19.0	0.4	4.2	0.4	N	A
2004-13 2	<i>Striatolamia</i>	7.3	-11.2	19.3	0.5	10.1	0.4	9.2	0.3	Y	A
2004-13 3	<i>Striatolamia</i>	17.9	-12.0	18.5	0.2	9.4	0.1	9.2	0.7	Y	A
2004-13 4	<i>Striatolamia</i>	18.4	-12.0	18.5	0.5	10.3	0.5	8.2	0.3	Y	A
2004-15 1*	<i>Carcharias</i>	15.2	-10.7	19.9	0.1	9.2	0.1	10.7	0.5	Y	A
2004-15 2	<i>Striatolamia</i>	17.3	-11.5	19.0	0.3	9.4	0.5	9.5	0.6	Y	A
2004-15 3	<i>Striatolamia</i>	20.1	-11.5	19.0	0.3	10.0	0.2	9.0	0.2	Y	A
2004-15 4	<i>Carcharias</i>	16.2	-10.7	19.8	0.1	11.6	0.7	8.2	0.7	Y	L
2004-15 5*	<i>Carcharias</i>	22.6	-9.5	21.0	0.2	15.5	0.2	5.5	0.1	N	A
2004-15 6	<i>Carcharias</i>	20.4	-12.8	17.7	0.2	9.5	0.7	8.1	0.5	Y	A
2004-15 7	§	7.2	-10.8	19.7	0.3	10.2	0.1	9.5	0.4	Y	P
2004-15 8	<i>Striatolamia</i>	8.3	-9.4	21.1	0.2	9.7	0.2	11.5	0.7	Y	A
2004-15 E (a)	§		-11.7	18.8	0.1					Y	U
2004-15 E (b)	§		-12.8	17.7	0.3	11.7	0.1	6.0	0.3	N	U
2004-15 F	§		-11.2	19.3	0.1					Y	U
2004-31 2*	<i>Carcharias</i>	10.9	-12.4	18.1	0.2	11.1	0.5	6.9	0.1	N	A
2004-31 3	<i>Carcharias</i>	20.4	-11.3	19.2	0.2					Y	L
2004-31 E	§		-11.7	18.8	0.0	9.4	0.5	9.4	0.2	Y	U
2004-31 F	§		-10.3	20.2	0.1	9.2	0.0	11.0	0.5	Y	U
sharktic 1	<i>Carcharias</i>	16.3	-10.1	20.4	0.2	10.6	0.7	9.8	0.1	Y	A
sharktic 2*	<i>Striatolamia</i>	15.2	-8.9	21.6	0.2	11.5	0.1	10.1	0.7	Y	A
sharktic 3	<i>Carcharias</i>	7.5	-10.4	20.2	0.3	11.5	0.2	8.7	0.3	Y	L
sharktic 4	<i>Striatolamia</i>	9.8	-9.1	21.4	0.1	12.5	0.3	8.9	0.4	Y	A

sharktic 5	<i>Carcharias</i>	10.2	-9.3	21.2	0.2	12.7	0.3	8.5	0.3	Y	A
sharktic 6	<i>Striatolamia</i>	12.7	-9.9	20.6	0.1	11.4	0.1	9.3	0.3	Y	A
sharktic 7	<i>Carcharias</i>	12.3	-9.2	21.4	0.2	12.3	0.1	9.1	0.1	Y	A
sharktic 9	<i>Striatolamia</i>	7.2	-9.4	21.2	0.1					Y	A
sharktic 13	<i>Striatolamia</i>	8.3	-11.9	18.6	0.1					Y	L
sharktic E <sup>‡</sup>	<i>Carcharias</i>		-11.1	19.4	0.2	11.8	0.4	7.6	0.1	Y	U
sharktic F	<i>Striatolamia</i>		-10.8	19.7	0.1	11.1	0.3	8.6	0.4	Y	U
Average			-10.7	19.8		10.6		9.1			
SD			1.1	1.1		1.2		1.0			

\* Notes shark for XRD analysis of enameloid

<sup>‡</sup> Notes shark tooth for two XRD analyses: E was the altered root and inner tooth whereas E2 was the enameloid

§ Genus cannot be determined because tooth was crushed before identification

<sup>a</sup> Carbonates analyzed on a gas bench; 1 $\sigma$  determined from 6 peaks within each analysis

<sup>b</sup> Phosphates analyzed on a TCEA and 1 $\sigma$  determined from triplicate analyses of the same sample as is standard practice (i.e., Tutken et al. 2006)

**Table DR2: Modern *C. taurus*  $\delta^{18}\text{O}_{\text{CO}_3}$  values**

Identifier	Total length (cm)	Sex	$\delta^{18}\text{O}_{\text{CO}_3}$ (VPDB, ‰)	1 $\sigma$
ST12-157m CO	205	M	1.2	0.3
ST12-175f CO	272	F	0.2	0.3
ST12-191m CO	251	M	-0.6	0.3
ST12-137m CO	240	M	0.7	0.4
ST12-130m CO	228	M	2.5	0.4
ST12-190m CO	212	M	3.1	0.2
ST12-216f CO	204	F	0.0	0.3
ST12-128f CO	170	F	-1.1	0.2
ST12-220f CO	161	F	-1.4	0.3
ST12-118f CO	152	F	2.0	0.4
ST12-151m CO	192	M	1.5	0.2
ST12-154f CO	131	F	1.1	0.3
ST12-20f CO		F	-0.9	0.2
ST12-089m CO	182	M	-0.6	0.2
ST12-179m CO	170	M	-1.1	0.2
ST12-223m CO	155	M	1.9	0.3
ST12-210m CO	139	M	2.2	0.1
ST12-141f CO	260	F	-0.3	0.2
ST12-139f CO	244	F	2.1	0.4

**Table DR3: Crystallinity index values for analyzed teeth and references.**

Sample ID	Material type	CI	H[211]	H[112]	H[300]	H[202]
2004-15 1	Eocene Arctic enameloid	1.03	98.5	16.25	62.25	23
2004-15_5	Eocene Arctic enameloid	1.42	137.5	56.04	102.49	36.46
2004-31_2	Eocene Arctic enameloid	1.24	154.38	62.08	95.42	34.58
sharktic 2	Eocene Arctic enameloid	1.49	103.96	62.28	65.42	27.5
sharktic E	Eocene Arctic Root/Dentine	0.54	57	10.25	13.1	7.25
sharktic E2	Eocene Arctic enameloid	1.52	54.25	8.25	67	7.25
sharktic F	Eocene Arctic enameloid	1.48	139	11.75	177	17
ST12-207	Modern enameloid	1.6	114.25	4.5	163.5	15.5
blue 1	Modern enameloid	1.42	94.17	35.42	67.7	26.04
Calcium Phosphate Hydroxide	Reference standard	1.36	94.34	53.38	53.49	21.71
Calcium Fluoride Phosphate	Reference standard	1.14	94.48	32.26	52.55	23.32
Calcium Carbonate Phosphate Fluoride Hydroxide	Reference standard	1.64	76.62	21.11	93.54	11.21
Calcium Chloride Phosphate	Reference standard	0.99	94.68	0	93.62	0.29

**Table DR4: Data description and model prior parameters (distribution shown in parenthesis).** Citations for Eocene model variables are given in text. Salinity prior for all models was 0 – 40 PSU (uniform distribution).

<b>Model variation</b>	<b><math>\delta^{18}\text{O}_{\text{CO}_3}</math> (‰, VPDB)</b>	<b>Temperature (°C)</b>	<b>Freshwater <math>\delta^{18}\text{O}</math> (‰, VSMOW)</b>
Eocene Arctic sand tiger sharks (this study)	Mean = -10.7 1 $\sigma$ = 1.1 (normal)	8 – 13 (uniform)	-20.3 – -17.5 (uniform)
Eocene warm Arctic sand tiger sharks (this study)	Mean = -10.7 1 $\sigma$ = 1.1 (normal)	16.5 – 19 (uniform)	-20.3 – -17.5 (uniform)
Lomonosov Ridge fish bone (Waddell and Moore 2008)	Mean = -4.9 1 $\sigma$ = 1.0 (normal)	9 – 15 (uniform)	-20 – -15 (uniform)
Extant <i>C. taurus</i> (this study)	Mean = -0.7 1 $\sigma$ = 1.1 (normal)	12 – 16 (uniform) <sup>1</sup>	-8 – -6.9 (uniform) <sup>2</sup>

<sup>1</sup>(Richardson and Schmals, 2006)

<sup>2</sup>(Khim and Krantz, 1996)

**Table DR5: Posterior parameter estimates (medians with 95% credible intervals in parenthesis).**

<b>Model variation</b>	<b>Temp. (°C)</b>	<b>Freshwater <math>\delta^{18}\text{O}</math> (‰, VSMOW)</b>	<b>Salinity (PSU)</b>	<b><math>\sigma^2</math></b>	<b><math>\beta_0</math></b>	<b><math>\beta_1</math></b>	<b><math>V^2</math></b>
Eocene Arctic	10.5 (8.1, 12.9)	-18.8 (-20.2, -17.6)	12.7 (10.3, 14.9)	1.6 (1.0, 2.7)	0.40 (-0.22, 0.98)	-35.4 (-36.6, -34.1)	0.6 (0.4, 1.0)
Eocene warm Arctic	17.5 (16.6, 18.9)	-18.9 (-20.2, -17.6)	15.8 (13.8, 17.7)	1.6 (1.0, 2.9)	0.40 (-0.21, 1.00)	-35.3 (-36.6, -33.9)	0.6 (0.4, 1.1)
Waddell and Moore (2008)	12.0 (9.2, 14.9)	-17.4 (-19.8, -15.1)	23.4 (20.4, 25.7)	1.3 (0.8, 2.2)	0.42 (-0.13, -0.95)	-35.4 (-36.6, -34.3)	0.6 (0.4, 1.0)
Extant <i>C. taurus</i>	13.9 (12.1, 15.9)	-7.4 (-8.0, -6.9)	34.9 (31.1, 38.7)	2.3 (1.4, 4.0)	0.4 (-.21, 0.99)	-35.4 (-36.5, -34.2)	0.5 (0.4, 1.0)

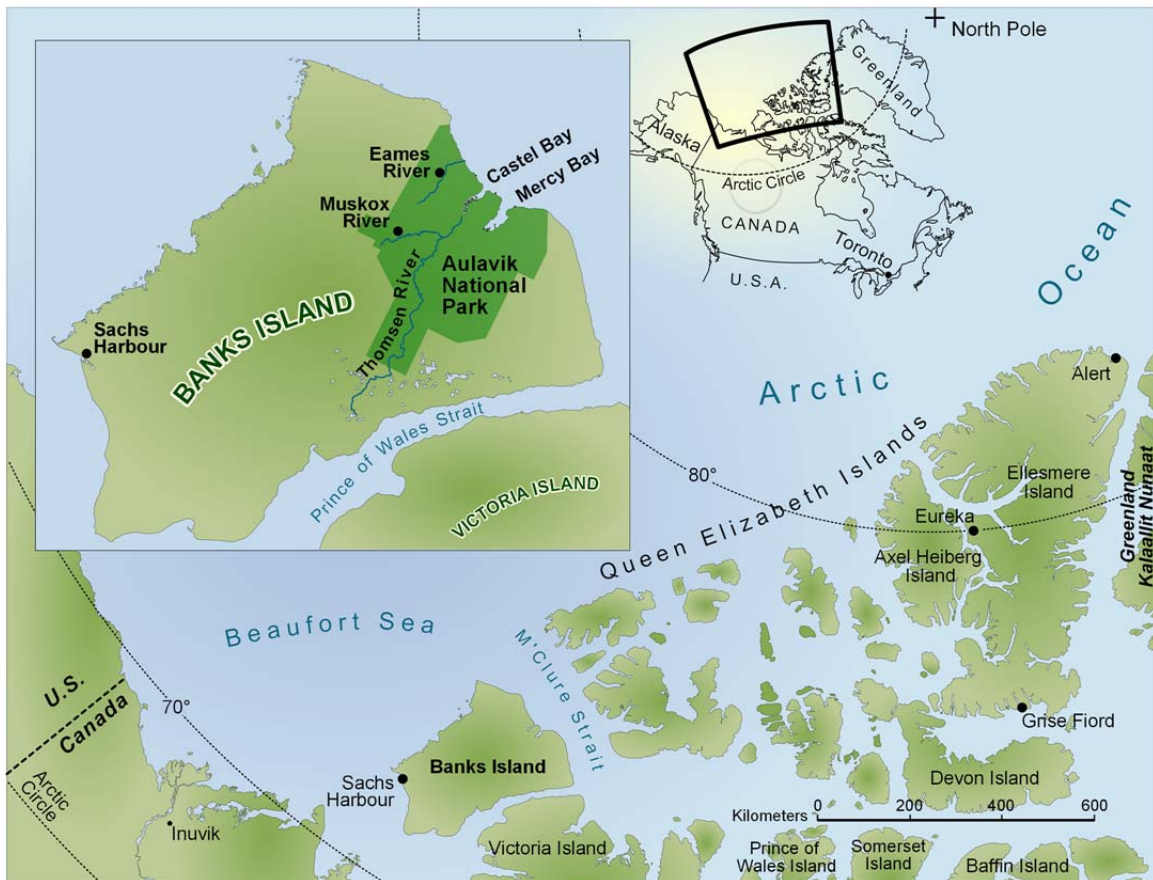


**Figure DR1. Map of Canadian Arctic vertebrate fossil localities.** Eocene sand tiger shark teeth were found on Banks Island (highlighted in inset) at Muskox and Eames River localities within Aulavik National Park.

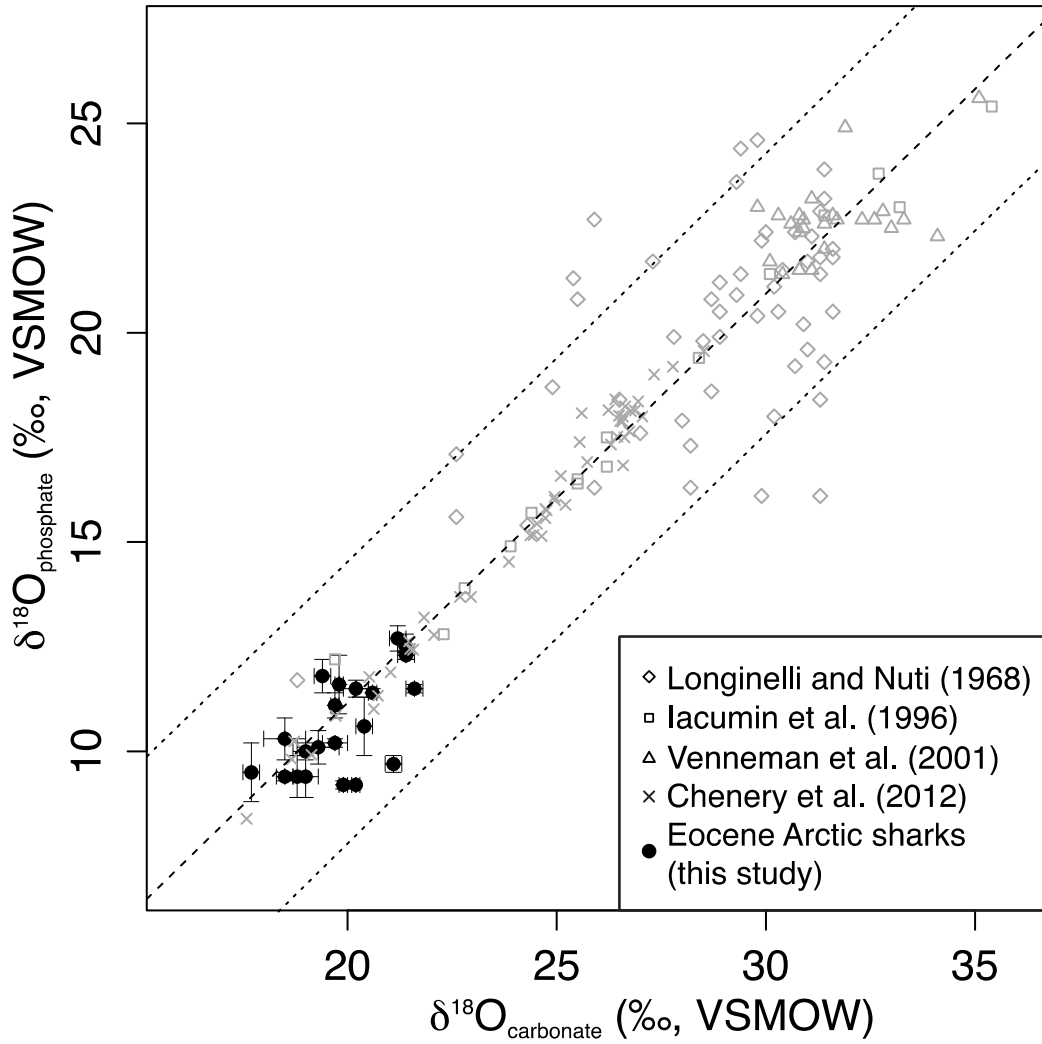


**Figure DR2. Comparison of  $\delta^{18}\text{O}$  values from carbonate and phosphate across three studies.** Data used for the linear regression (dashed line) are from Longinelli and Nuti (1968), Iacumin et al. (1996), and Venneman et al. (2001), shown in open symbols. The 95% prediction interval for this regression is shown with dotted lines. Data from Eocene Arctic sand tiger sharks in this study are shown as filled black circles (error bars represent  $1\sigma$ ).

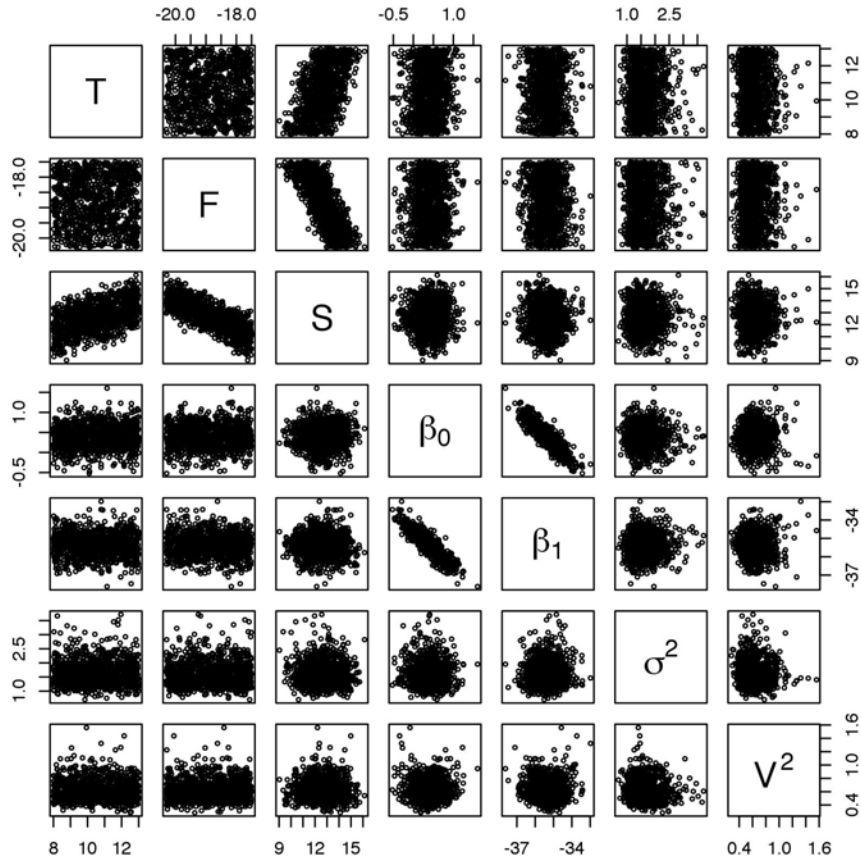


**Figure DR3: Covariation in model parameter estimates for every 100<sup>th</sup> iteration of the Gibbs sampler based on the Eocene data.** This example is characteristic of the correlations observed for each of the three datasets analyzed (see Table DR3 and DR4).

## References Cited

- Bassett, D., Macleod, K.G., Miller, J.F., And Ethington, R.L., 2007, Oxygen Isotopic Composition of Biogenic Phosphate and the Temperature of Early Ordovician Seawater: *Palaios*, v. 22, no. 1, p. 98–103, doi: 10.2110/palo.2005.p05-089r.
- Clark, J.S., 2007, *Models for Ecological Data*. Princeton University Press, Princeton, NJ, USA. p. 617
- Chenery, C.A., Pashley, V., Lamb, A.L., Sloane, H.J., and Evans, J.A., 2012, The oxygen isotope relationship between the phosphate and structural carbonate fractions of human bioapatite: *Rapid Communications in Mass Spectrometry*, v. 26, no. 3, p. 309–319, doi: 10.1002/rcm.5331.
- Iacumin, P., Bianucci, G., and Longinelli, A., 1992, Oxygen and carbon isotopic composition of fish otoliths: *Marine Biology*, v. 113, no. 4, p. 537–542.
- Khim, B.-K., and Krantz, D.E., 1996, Oxygen isotopic identity of the Delaware Coastal Current: *Journal of Geophysical Research*, v. 101, no. C7, p. 16509–16–514.
- LeGrande, A.N., and G.A. Schmidt, 2006, Global gridded data set of the oxygen isotopic composition in seawater: *Geophysical Research Letters*, v. 33, L12604, doi:10.1029/2006GL026011.
- Longinelli, A., and Nuti, S., 1968, Oxygen-isotope ratios in phosphate from fossil marine organisms: *Science*, v. 160, no. 3830, p. 879–882.
- Person, A., Bocherens, H., Saliège, J.F., Paris, F., Zeitoun, V., and Gérard, M., 1995, Early diagenetic evolution of bone phosphate: an X-ray diffractometry analysis: *Journal of Archaeological Science*, v. 22, no. 2, p. 211–221.
- Posner, A.S., Blumental, N.C., and Betts, F., 1984, Chemistry and Structure of Precipitated Hydroxyapatites, *in* Nriagu, J.O. and Moore, P.B. eds., *Phosphate Minerals*, Springer-Verlag, New York, p. 330–350.
- Richardson, P.H., and Schmals, R.A., 2006, Restoration of CTD data from the 1984-1985 Delaware River and Bay circulation study: *Coast Survey Development Laboratory* 5.
- Tutken, T., Vennemann, T.W., Janz, H., and Heizmann, E.P.J., 2006, Palaeoenvironment and palaeoclimate of the Middle Miocene lake in the Steinheim basin, SW Germany: A reconstruction from C, O, and Sr isotopes of fossil remains: *Palaeogeography, Palaeoclimatology, Palaeoecology*, v. 241, no. 3-4, p. 457–491, doi:

10.1016/j.palaeo.2006.04.007.

- Vennemann, T.W., Fricke, H.C., Blake, R.E., Oneil, J.R., and Colman, A., 2002, Oxygen isotope analysis of phosphates: a comparison of techniques for analysis of  $\text{Ag}_3\text{PO}_4$ : *Chemical Geology*, v. 185, no. 3-4, p. 321–336.
- Vennemann, T., Hegner, E., Cliff, G., and Benz, G., 2001, Isotopic composition of recent shark teeth as a proxy for environmental conditions: *Geochimica et Cosmochimica Acta*, v. 65, no. 10, p. 1583–1599.
- Waddell, L. M., and Moore, T.C., 2008, Salinity of the Eocene Arctic Ocean from oxygen isotope analysis of fish bone carbonate: *Paleoceanography*, v. 23, PA1S12, doi:10.1029/2007PA001451.
- Wiedemann-Bidlack, F.B., Colman, A.S., and Fogel, M.L., 2008, Phosphate oxygen isotope analysis on microsamples of bioapatite: removal of organic contamination and minimization of sample size: *Rapid Communications in Mass Spectrometry*, v. 22, no. 12, p. 1807–1816, doi: 10.1002/rcm.3553.